NRL Report 5215

UNCLASSIFIED

PROJECT VANGUARD REPORT NO. 33

MINITRACK REPORT NO. 7

CALIBRATING THE MARK II MINITRACK SYSTEM WITH RADIO STARS AS SIGNAL SOURCES

V. R. Simas and LTJG G. C. Kronmiller, Jr., U.S.N.

Radio Tracking Branch
Project Vanguard

October 17, 1958

U. S. NAVAL RESEARCH LABORATORY
Washington, D.C.

PREVIOUS REPORTS IN THE MINITRACK REPORT SERIES

NRL Report 4995, "Project Vanguard Report No. 18, Minitrack Report No. 1; Phase Measurement," by C. A. Schroeder, C. H. Looney, Jr., and H. E. Carpenter, Jr., July 26, 1957

NRL Report 5035, "Project Vanguard Report No. 21, Minitrack Report No. 2; The Mark II Minitrack System," by R. L. Easton, September 12, 1957

NRL Report 5055, "Project Vanguard Report No. 23, Minitrack Report No. 3; Receiver System," by V. R. Simas and C. A. Bartholomew, December 6, 1957

NRL Report 5065, "Project Vanguard Report No. 24, Minitrack Report No. 4; "The Satellite Telemetry Receiver System," by V. R. Simas, January 20, 1958

NRL Report 5198, "Project Vanguard Report No. 32, Minitrack Report No. 5; Minitrack Data for the Artificial Earth Satellites 1958 Alpha and 1958 Beta from 7 May to 20 May 1958," compiled by W. M. Hocking, September 22, 1958

NRL Report 5217, "Project Vanguard Report No. 35, Minitrack Report No. 6; "The Vanguard Satellite Command Receiver," by D. S. Hepler, September 30, 1958

UNCLASSIFIED

CONTENTS

Abstract	ii
Problem Status	ii
Authorization	ii
INTRODUCTION	1
OPERATIONAL ANALYSIS OF THE SYSTEM	1
RADIO STAR CALIBRATION	7
Sources Employed	7
Use of Star Records	9
Astronomical Calculation of Star Positions	10
System Measurement of Star Positions	12
RESULTS AND CONCLUSIONS	14
ACKNOWLEDGMENTS	16
Appendix A - DAILY TRACKING DATA FOR CASSIOPEIA, CYGNUS, AND TAURUS, 24 JANUARY - 10 APRIL 1957	23

ABSTRACT

The Mark II Minitrack System is described briefly and an operational analysis is made. A means of external calibration of the system by tracking radio stars is described and illustrated. Results obtained by this method are presented and compared with results obtained by the complex but more precise method used in calibrating Prime Minitrack stations. It is shown that the tracking of radio stars does in fact provide an adequate system calibration if sufficient data are taken.

PROBLEM STATUS

This is an interim report on one phase of the problem, work is continuing.

AUTHORIZATION

NRL Problem A02-86
Project No. NR 579-000

Manuscript submitted 1 October 1958

UNCLASSIFIED

ERRATA SHEET
for
NRL Report 5198
(Project Vanguard Report No. 32)

Equation (4) on page 6 of subject report is in error. Please cut out the corrected Equation below, moisten and paste in the report, covering the erroneous equation.

$$b_c = C_o + C_1 a_o + C_2 b_o + C_3 a_o b_o + C_4 a_o^2$$

$$+ C_5 b_o^2 + C_6 b_o^3 + C_7 \sin "b_o" + C_8 \cos "b_o";$$

UNCLASSIFIED

CALIBRATING THE MARK II MINITRACK SYSTEM WITH RADIO STARS AS SIGNAL SOURCES

INTRODUCTION

The Mark II Minitrack System,* whose function is primarily the tracking of artificial satellites, has also been designed for the tracking of radio stars. The ephemerides (position schedules) of several of these radio-noise sources are established with sufficient accuracy to permit their use in calibrating Mark II Minitrack stations. At the same time valuable information may be gained concerning the effects of the ionosphere and troposphere on these signals from outer space.

The allowable tracking error for the Mark II stations is about 30 seconds of arc. It is probable, however, that the antennas and lines cannot be constructed and installed with sufficient precision to guarantee an error of less than about 100 seconds of arc. Therefore the stations must be externally calibrated if the finer accuracy is to be attained. Calibrating the station consists of comparing the actual position of a signal source with its position as determined by the station. Since a satellite-tracking system is only concerned with elevated signal sources, it is necessary that the calibration source pass over the station.

A very accurate aircraft-borne system is employed in calibrating the Prime Minitrack stations and was also used to check the radio star calibrating procedure described in this report. The position of the aircraft is determined very accurately by a complex system which includes time and tracking signals telemetered from the ground to the plane, and a ground camera equipped with a sidereal drive to photograph a flashing light on the plane against a star background. Because the successful use of this system depends upon clear weather and employs many complicated devices, a simpler calibrating system is most desirable for the Mark II Minitrack System, even though it may not provide so accurate a calibration.

The existence of radio stars provides a means of calibration which, although possessing certain deficiencies, permits the requisite accuracy to be attained.

OPERATIONAL ANALYSIS OF THE SYSTEM

The Mark II Minitrack System is a radio interferometer operating at 108 Mc, the frequency of the satellite-borne Minitrack transmitter. The geometry of this system is shown in Fig. 1. The points A_1 and A_2 represent a pair of antennas required for a single angle measurement. Because the antenna separation d is negligible compared to the distance to the signal source, the signals to the two antennas can be assumed to arrive in parallel paths. Thus the signals at A_1 and P are equal in phase since the line A_1P is perpendicular to the signal path. Because the wave arriving at A_2 travels an additional distance $PA_2 = S$ there will, in general, be a phase difference between the signals at the two antennas; this phase difference, ϕ, is measured by the Mark II Minitrack system.

*Easton, Roger L., "Project Vanguard Report No. 21, Minitrack Report No. 2, The Mark II Minitrack System," NRL Report 5035, 12 September 1957.

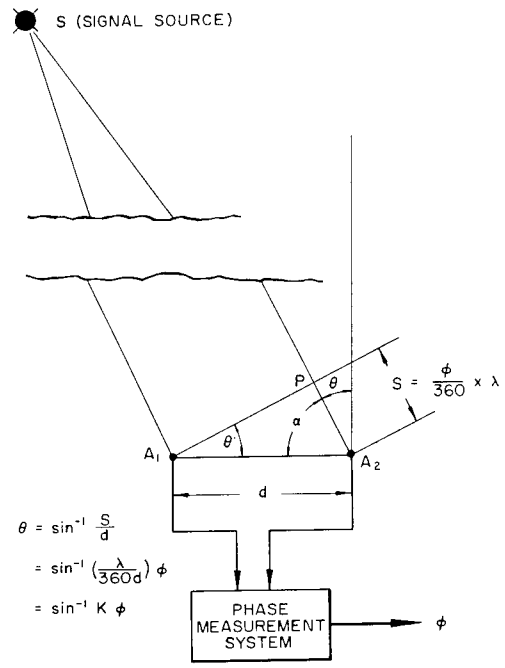

Figure 1 - Geometry of Mark II Minitrack system

The distance S is given by the expression $\lambda\phi/360$, where λ is the wavelength in the air at the signal frequency. The angle θ is the direction of the signal source with respect to the station in the plane defined by the triangle SA_1A_2. From the figure,

$$\theta = \sin^{-1} \frac{S}{d}$$

$$= \sin^{-1} \frac{\lambda\phi}{360\ d} .$$

Since the factor $\lambda\phi/360\ d$ is a constant for any particular system,

$$\theta = \sin^{-1} K\phi .$$

Thus θ is a function of the phase angle ϕ only. A second angle measurement by means of antennas oriented in a direction differing from that of A_1 and A_2 will establish the direction of the source in a second plane. The information from both measurements determines the actual position vector of the source.

In the foregoing discussion certain matters have been excluded in the interest of simplicity. Among these is the fact that the distance S may consist of more than one wavelength. The Mark II Minitrack system is not designed to determine directly the integral number of wavelengths in S, and consequently provides information which is, in general, ambiguous. In the Prime Minitrack System this ambiguity is resolved by means of additional angle measurements from antenna pairs with reduced spacing so that S cannot exceed a single wavelength within the beamwidth of the antennas. However, because the system accuracy is directly proportional to d within limits, the longer baseline lengths are also necessary.

The Mark II Minitrack system is a basic type of radio interferometer in which the signals from the antennas are directly combined. The signals can be combined by connecting the antenna transmission lines directly as shown in Fig. 2, which illustrates the

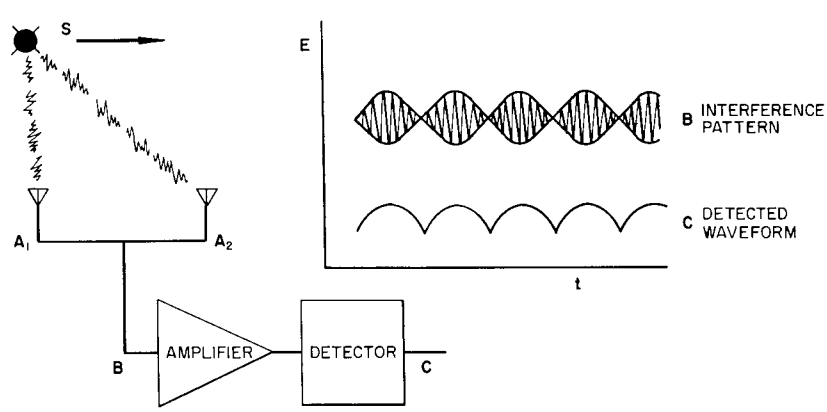

Figure 2 - Basic radio-interferometer theory

UNCLASSIFIED

basic radio-interferometer theory. As the signal source passes over the station the signals from the antennas, which have a spacing of many wavelengths, will alternately interfere constructively and destructively as the phase difference changes from an even to an odd number of half-wavelengths.

The mathematical expression for the waveform e_B at B is derived in the following manner: Let the signal from the source be represented by $E \cos \omega t$. Then at the points A_1 and P (Fig. 1), the signal is

$$e_{A_1} = E \cos \left(\omega t - \frac{2\pi r}{\lambda}\right),$$

where r is the range from the antenna to the source. The signal at A_2 is identical to that at A_1 except for an additional phase shift of $2\pi S/\lambda$:

$$e_{A_2} = E \cos \left(\omega t - \frac{2\pi r}{\lambda} - \frac{2\pi S}{\lambda}\right),$$

or, since $S = d \sin \theta$,

$$e_{A_2} = E \cos \left(\omega t - \frac{2\pi r}{\lambda} - \frac{2\pi d \sin \theta}{\lambda}\right).$$

For simplification, let

$$a = \omega t - \frac{2\pi r}{\lambda},$$

$$b = \frac{2\pi d \sin \theta}{\lambda};$$

then

$$e_{A_1} = E \cos a,$$

$$e_{A_2} = E \cos (a-b).$$

The interferometer combines these voltages (Fig. 2) so that if the line lengths are equal

$$e_B = E \cos a + E \cos (a-b);$$

expanded and simplified, this is

$$e_B = 2E \cos \left(a - \frac{b}{2}\right) \cos \frac{b}{2}.$$

The argument $(a-b/2)$ contains the rf term, while $b/2$ is a low-frequency amplitude-modulating term representing the difference in phase. The interference pattern shown in Fig. 2 is a plot of this expression, showing the manner in which the phase information is converted to an amplitude-modulated signal. This signal is amplified and detected, resulting in the pattern at C. The tracking data are obtained by noting the times at which the nulls occur, which times are of course related to the position of the signal source. Thus the system does not provide continuous information; however the signal course positions at discrete points corresponding to the nulls are usually adequate to establish the required tracking information.

A block diagram of the Mark II Minitrack System is shown in Fig. 3. In this system the signals from the antennas are combined by means of a hybrid junction instead of by

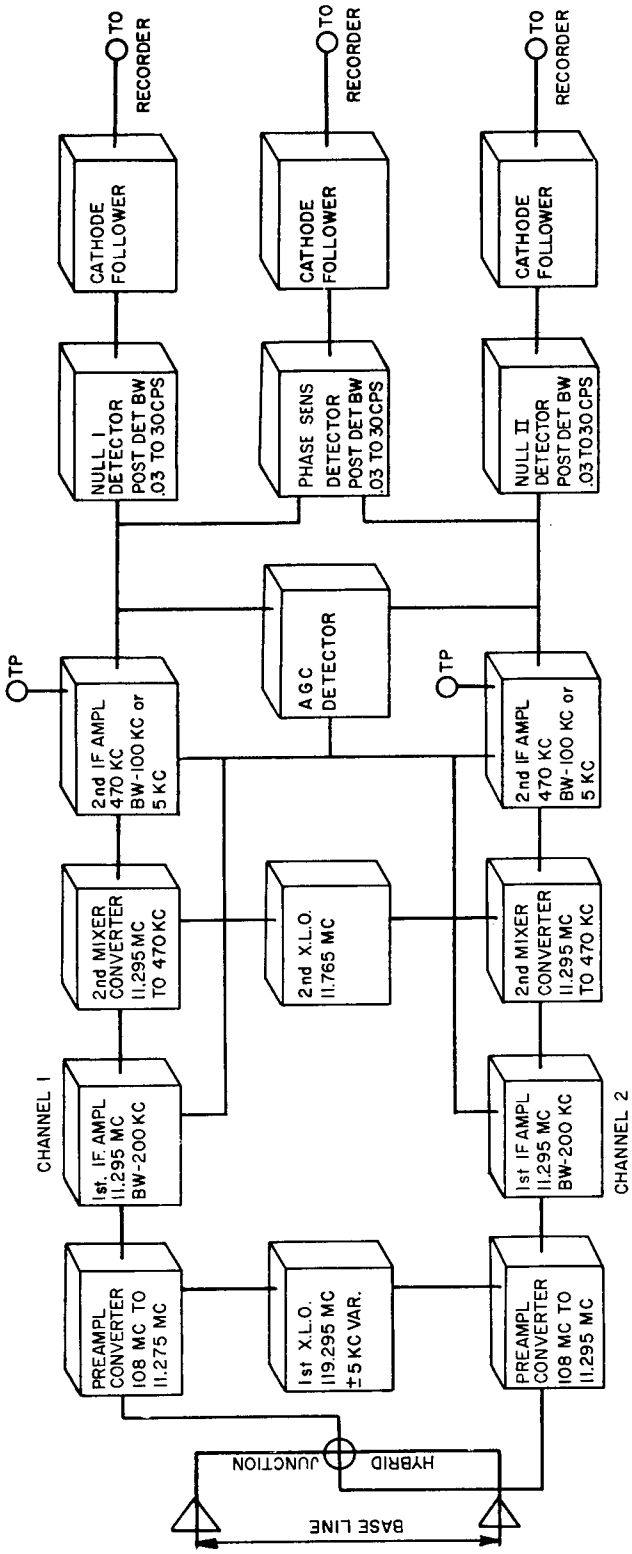

Figure 3 - Mark II Minitrack System

UNCLASSIFIED

connecting the transmission lines as was previously discussed. The hybrid junction has two outputs, each of which supplies half the incoming signal power to the impedance-matched low-noise frequency converters. This is an improvement over the directly connected system in which part of the received power is dissipated in the source impedance of each antenna circuit. Although the outputs of the individual channels, called the "null outputs," have the same signal-to-noise ratio with either method, the hybrid connection provides twice as many nulls from which to extract the tracking information. The principal improvement, however, is derived from the phase-sensitive detector which combines the outputs of the two channels and detects the resulting signal in a manner that provides a 3-db increase in the output signal-to-noise ratio in addition to making the system insensitive to input-signal amplitude changes.

The receivers in the two channels are conventional double-conversion units using the two crystal-controlled local oscillators in common. The AGC bus is common to both units and is controlled by the receiver having the higher output at a particular time. The 108-Mc input signal is first amplified by a preamplifier with a noise figure of about 4 db, then converted in frequency to 11.295 Mc by means of the 119.295-Mc local oscillator. After two stages of amplification the first i-f signal is converted to a 470-kc signal by means of the second local oscillator frequency of 11.765 Mc. After three stages of amplification the signal is ready for detection in the three types of detectors—the null detector, the AGC detector, and the phase-sensitive detector. The passband of the system is determined by the second i-f strip, which is provided with means for switching from the 5 kc required when the input signal is obtained from a man-made source to the 100 kc required when the input signal is obtained from a noise source such as a radio star.

The inputs to the phase-sensitive detector are phase-coherent because of the common local oscillators in the two receiver channels. A phase shifter in one of these channels provides means for adjusting the phase difference of the two inputs to zero or 180 degrees, depending upon the particular part of the interference cycle considered. The output waveform of the phase-sensitive detector is shown in Fig. 4 together with the null outputs. Note that when the output of channel 1 is a maximum that of channel 2 is a minimum, and vice versa. When either channel is at a null, the phase-sensitive detector is at zero, or what is called the "crossover." These voltages are connected to the input of a visual recorder and are the actual recorded patterns from which tracking information is obtained. The time interval between crossovers is about 1/2 second for a satellite signal source at an altitude of about 300 miles and increases for higher altitudes. Stellar sources have much lower angular velocities which are due entirely to the Earth's rotation; the resulting interval between crossovers is 2 minutes for sources on the celestial equator and increases as the cosine of the declination. The post-detection bandwidths of the three outputs are switched to values approximately ten times the crossover frequency. The phase shift resulting from the integrating networks is thus about 6 degrees* and the data should be compensated accordingly.

The antennas used in the observations described herein were those of the 500-foot east-west baseline of the

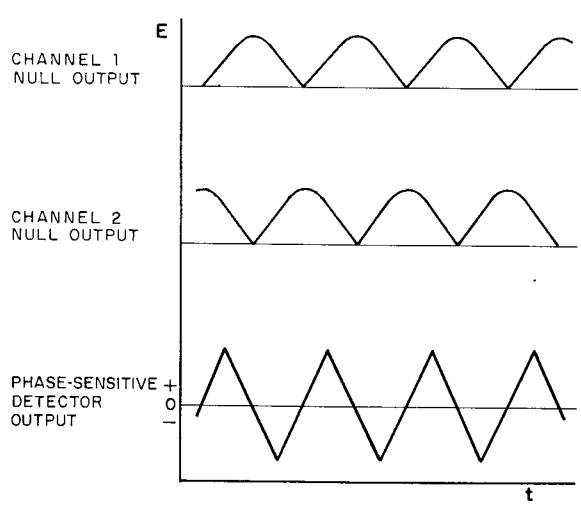

Figure 4 - Mark II Minitrack output waveform

*See p. 13

Prime Minitrack station located at Blossom Point, Maryland. Their physical spacing was 500 feet ±1/8 inch and their difference in elevation was adjusted to less than 1/8 inch. Each of the two antenna arrays is composed of eight radiating elements (Fig. 5). The long dimension of the array is oriented east and west; the antenna beam is therefore wide (100 degrees) in the north-south direction and narrow (10 degrees) in the east-west direction with the main lobe, of course, oriented vertically. The position of the midpoint between the two antennas is 38° 25' 49.628" north latitude and 77° 5' 11.775" west longitude.

The four outputs of the system, i.e., the two nulls, the output of the phase-sensitive detector, and the AGC voltage which indicates the input signal level, are fed into an eight-channel hot-pen visual recorder. A recording made during an aircraft calibration run is shown in Fig. 6. The plane's altitude and speed (15,000 ft and 175 mph) were such as to

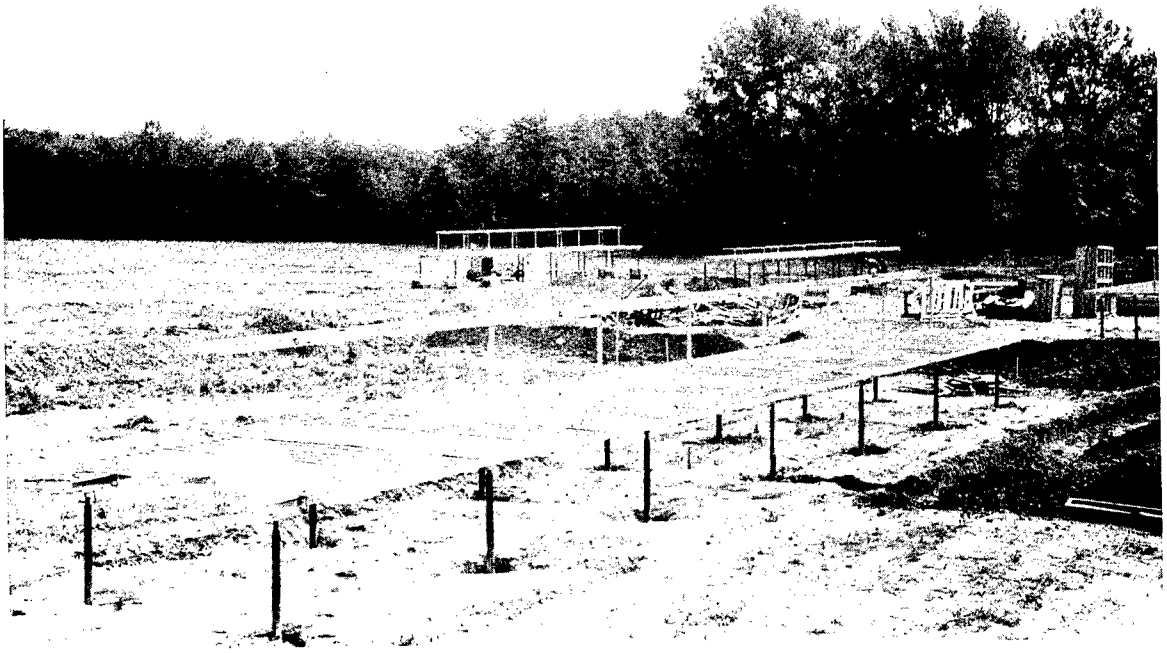

Figure 5 - Prime Minitrack antenna array at Blossom Point

Figure 6 - Mark II Minitrack recording of calibration flight

UNCLASSIFIED

simulate the approximate angular velocity of an artificial satellite. Channel 1 shows the AGC voltage (input signal level) with the increase in the downward direction. Channels 2 and 3 show the corresponding null outputs with the nulls pointing upward; the flattening at the bottoms of these waves is due to the recorder limits. Channel 4 shows the output of the phase-sensitive detector, which is almost a perfect sine wave resulting from the integration of the triangular detected wave. Channels 5, 6, and 7 were not used. Channel 8 again shows the output of the phase-sensitive detector, this time with the gain of the recorder amplifier increased to a point where the recorder limits flatten the tops and bottoms of the wave. The slope in the phase-sensitive detector pattern is due to the relatively low altitude of the aircraft, which results in the source appearing in different parts of the main lobes of the two antennas.

Extremely accurate timing marks are placed on the record as shown by the trace marked 9. The time is determined by subtracting 2 from the first of five digits and 1 from each of the other four. Thus the first complete timing indication toward the left of Fig. 6 is from left to right, 4, 1, 6, 8, 6. Subtracting the required numbers results in 2, 0, 5, 7, 5, or 20 hours, 57.5 minutes, or 8:57 and 30 seconds p.m. Eastern Standard Time. This time should correspond to the beginning of the first digit. Actually it refers to 3 milliseconds before the beginning indication, owing to the inertia of the recording pen mechanism.

The coded time marks are derived from a very accurate time standard unit which is periodically corrected by comparison with WWV time ticks. This unit derives its accuracy from a very stable 100-kc oscillator whose output is divided in countdown circuits. The resulting 1-second pulses are conveyed to a digital clock which codes the information and applies the result to the recorder.

RADIO STAR CALIBRATION

Sources Employed

The five radio sources from which the greatest radio energy is received are listed in Table 1 along with their positions, sizes, and flux densities. The energy is in the form of random fluctuations spread over a wide range of the electromagnetic spectrum including the radio portion. The level varies, increasing in general at the lower frequencies. The experimentally determined signal-to-noise ratio of the recorded signals from

TABLE 1
Positions of Radio Stars*

Constellation	Position (1950 Epoch)		Frequency (Mc)	Flux Density $\left(\frac{\text{Watts}}{\text{m}^2\ \text{cps}}\right)$	Angular Size
	Right Ascension	Declination			
Cygnus	$19^h\ 57^m\ 45^s.3 \pm 1^s$	$40°\ 35' \pm 1'$	100	125×10^{-24}	$2'10'' \times 35''$
Cassiopeia	$23^h\ 21^m\ 12^s \pm 1^s$	$58°\ 32'.1 \pm 0'.7$	158	93×10^{-24}	$3' \times 4'$
Centaurus	$13^h\ 22^m\ 30^s \pm 4^s$	$-42°\ 46' \pm 2'$	100	18.5×10^{-24}	$3' \times 6\frac{1}{2}'$
Taurus	$05^h\ 31^m\ 29^s \pm 2\frac{1}{2}^s$	$22°\ 00' \pm 3'$	100	18.5×10^{-24}	$3\frac{1}{2}' \times 5\frac{1}{2}'$
Virgo	$12^h\ 28^m\ 15\frac{1}{2}^s \pm 2\frac{1}{2}^s$	$12°\ 44' \pm 6'$	100	12.5×10^{-24}	$2\frac{1}{2}' \times 5'$

*From The Astrophysical Journal, Volume 121, No. 1, January 1955.

Cassiopeia and Cygnus is in the neighborhood of 35 db, while that of the signals from Taurus is about 18 db. The input signal level from Taurus is only 10 db less than that from Cassiopeia; however it suffers a 17-db reduction in output signal-to-noise ratio through the corrupting effects of the second detector because of receiver noise superimposed on the signal. These signal-to-noise ratios might appear astoundingly good, considering the comparatively weak input signals; however, they are justified by the wide (100-kc) pre-detection bandwidth which encompasses a significant portion of the input power spectrum, and the narrow (0.03-cps) post-detection bandwidth which removes a great deal of noise by permitting only the extremely low frequencies to pass.

These sources, as listed in Table 1, are seen to be areas rather than the point sources usually attributed to stars. However, the effective radio centers of these sources are known quite precisely despite their extensive physical areas, as will be noted by the tolerances given for their radio positions.

Typical examples of the data from these radio stars obtained on 19 March 1957 are shown in Figs. 7, 8, and 9. These figures, unlike Fig. 6 which showed the complete pattern, show only a small part of the daily run. The portion selected is near the meridian crossing time for that day and is so positioned that the nulls and crossovers appear near the center of the figure. Relative signal strengths obtained from these sources are easily discernible in these figures. The Cassiopeia pattern shows very little noise, the Cygnus

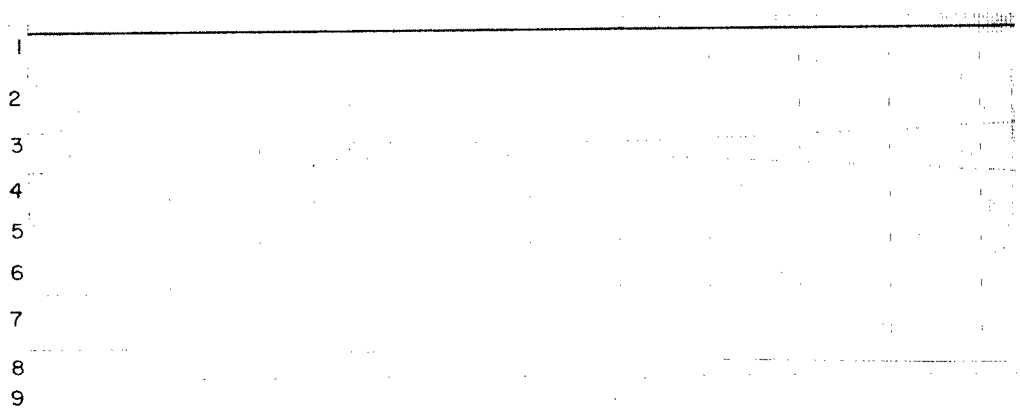

Figure 7 - Mark II Minitrack recording of Cassiopeia, 19 March 1957

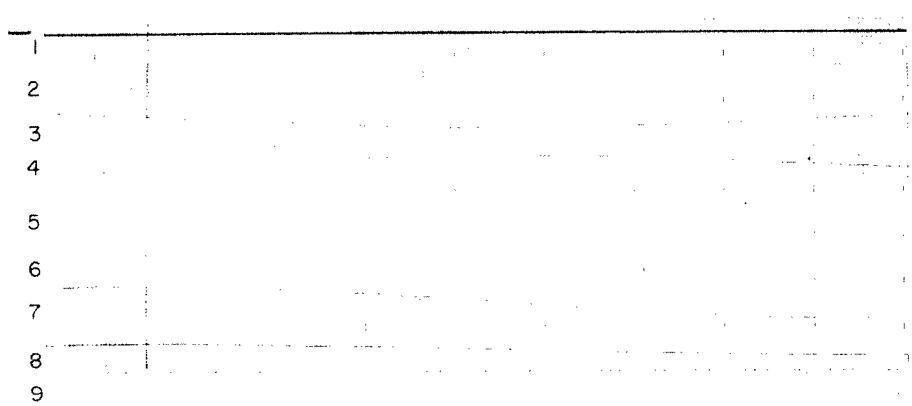

Figure 8 - Mark II Minitrack recording of Cygnus, 19 March 1957

UNCLASSIFIED

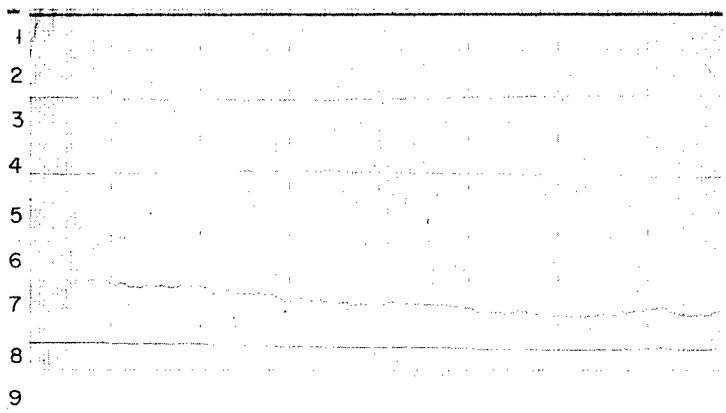

Figure 9 - Mark II Minitrack recording of Taurus, 19 March 1957

pattern shows a small increase in noise fluctuations, and the Taurus pattern shows a pronounced noisiness. However, the signal-to-noise ratio is still quite sufficient to permit the use of Taurus as a calibrating source.

Use of Star Records

The information extracted from these data is the times at which the output of the phase-sensitive detector equals zero, previously referred to as crossovers. A crossover occurs in time coincidence with a null on one channel and a maximum on the other. To analyze the data most expeditiously it is necessary to approximately center the phase-sensitive detector recording so that the crossover occurs near the mid-point of the record. Background radiation noise causes the pattern to shift its position so that sometimes it is necessary to compensate for this shift with a position control. The usual procedure is to position all the traces before the source being investigated comes within the main lobe of the antenna. The ensuing recorded pattern of the source then should appear approximately centered so that a reference line chosen near the center of the pattern is also close to the center of the recording channel. The reference line chosen is taken as the phase-sensitive detector "zero."

The system-derived meridian crossing time is determined by reading the time of the particular crossover designated zero. If the electrical line lengths from the antennas to their junction were exactly equal, the measured and computed meridian crossing times would agree exactly. The lines used for these observations were actually very nearly equal; therefore the zero crossover is established by choosing the crossover closest to the computed meridian crossing time. A rough corroboration of this method is obtained by observing the data during an entire transit. Because the main antenna lobe is symmetrical and quite narrow in the east-west direction, it is possible with practice to identify the zero crossover by observing the crossover between the maximum oscillographic pattern excursions.

The times corresponding to several crossovers on each side of the one designated zero are also compared to their computed times in order to exploit the data for this additional valuable information. The four data points prior to zenith and the five after zenith, together with the zero crossover, provide a total of ten points whose average is the measured meridian crossing time for the particular day. The crossover times are determined by laying a straight-edge on the patterns, thereby effectively decreasing the post-detection bandwidth even more. The crossover times are read to the nearest 0.1 second. A correction must be applied to the crossover times to compensate for the

delay in the electronic integrating circuits used to limit the post-detection bandwidth; this correction will be described presently. Visual integration, of course, requires no correction.

Astronomical Calculation of Star Positions

The non-astronomer should note that the stars appear earlier each day by 3 minutes, 55.9 seconds, which is the difference between mean solar and sidereal time. This difference results from the fact that the earth revolves around the sun in the same direction that it rotates about its axis, so that it rotates once less per year with respect to the sun than with respect to the star field. If these radio stars are to be used to calibrate the tracking stations it is necessary that their meridian crossing times (MCT) be accurately determined. Table 1 gives their positions for the 1950 Epoch; therefore in order to determine the MCT for a particular date it is necessary to adjust their ephemerides for the subsequent changes in the Earth's orientation.

The positions as listed in the Astrophysical Journal are given in terms of right ascension (R.A.) and declination (decl.). These are terms locating celestial bodies with respect to a point on the celestial sphere designated the vernal equinox. Because the orientation of the earth with respect to this point is also obtainable, i.e., the right ascension and declination, the meridian crossing time of a particular source can be determined.

To obtain star positions for years subsequent to 1950 it is necessary to add a small correction for each elapsed year. This correction is 3.07 + 1.34 sin(R.A.) tan(decl.) seconds per year. For Cassiopeia the correction is 2.69 seconds per year, or 18.9 seconds of time which must be added to the right ascension of Cassiopeia in order to correct its position for zero hours (0^h) Universal or Greenwich Meridian Time (U.T. or G.M.T.) 1 January 1957.

The apparent position of the star must now be computed for the particular day in question in the year 1957. Because of the precession and nutation of the earth and the aberration of the light and radio energy from the stars incident upon the earth it is not possible merely to extrapolate from the first day of the year to any particular day of the year. In order to compute the right ascension (in time) of a source for a particular day it is necessary to use the following equation* which corrects for the effects of precession, nutation, and aberration:

$$\alpha = \alpha_o + \tau\mu + Aa + Bb + Cc + Dd + E \text{ (in time).}$$

The first term, α_o, is the right ascension for 1 January 1957 at 0^h U.T. The second term, $\tau\mu$, is the proper motion of the star and is negligible. The quantities A, B, C, D and E are the Besselian Star Numbers given for every day of the year in a table of the American Ephemeris and Nautical Almanac. The quantities a, b, c, and d are Bessel's star constants given by

$$a = 3\overset{s}{.}07340 + 1\overset{s}{.}33613 (\sin \alpha_o \tan \delta_o), \qquad c = \frac{1}{15} (\cos \alpha_o \tan \delta_o),$$

$$b = \frac{1}{15} (\cos \alpha_o \tan \delta_o), \qquad d = \frac{1}{15} (\sin \alpha_o \sec \delta_o),$$

where δ_o is the declination for 1 January 1957 at 0^h U.T.

*The American Ephemeris and Nautical Almanac, 1957, p. 242.

UNCLASSIFIED

Thus, for Cassiopeia on 19 March 1957 the computation would be as follows:

$\alpha_o = 23^h\ 21^m\ 30^s.9$		$\delta_o = 58°\ 34'.4$
$a = +2^s.70794$	$A = +0.4900$	$Aa = +1^s.33$
$b = +0.10757$	$B = +5.00$	$Bb = +0^s.54$
$c = +0.12607$	$C = -18.77$	$Cc = 2^s.37$
$d = -0.02137$	$D = +0.67$	$Dd = -0^s.01$
		$= -0^s.51$

$E = +0^s.002$ and can be neglected. Hence,

$= 23^h\ 21^m\ 30^s.9 - 0^s.5 = 23^h\ 21^m\ 30^s.4.$

When the correct right ascension of the star source is known the meridian transit time can be determined. Although these calculations are routine in astronomy the novice may find the chart shown in Fig. 10 useful in this determination. The inner circle represents the earth viewed from above the north pole. The point marked 0 represents Greenwich and designates zero Universal Time (0^h U.T.). The vernal equinox is located with respect to Greenwich by the table on page 4 of the American Ephemeris and Nautical Almanac. The angle between the equinox and Greenwich, equal to the right ascension of the mean sun plus 12 hours, is read from the tables for the date in question (19 March 1957) as 11 hours 45 minutes 05.8 seconds of sidereal time. The vernal equinox (τ) is thus located on the chart. Cassiopeia is located on the chart by rotating counterlockwise from τ an angle equal to the right ascension of Cassiopeia, 23 hours 21 minutes 30.4 seconds. Blossom Point is located to the west of Greenwich a time corresponding to its longitude, or 05 hours 08 minutes 20.8 seconds. Because the stars move east to west (clockwise on the chart of Fig. 10) Cassiopeia will transit Greenwich in an interval of time equal to the angle between Cassiopeia and Greenwich, which is found by subtracting the right ascension of the mean sun plus 12 hours from the right ascension of Cassiopeia:

R.A. of Cass.:	R.A. $23^h\ 21^m\ 30^s.4$
R.A. mean sun + 12^h:	R.A. $11^h\ 45^m\ 05^s.8$
Greenwich transit of Cassiopeia, sidereal time:	$11^h\ 36^m\ 24^s.6$

The star will then transit Blossom Point after a time corresponding to the longitude of that station:

	$11^h\ 36^m\ 24^s.6$
	$05^h\ 08^m\ 20^s.8$
Cassiopeia transit of Blossom Point Sidereal Time:	$16^h\ 44^m\ 45^s.4$

To convert sidereal time into mean solar time it is necessary to add a small correction which can be determined from Table II

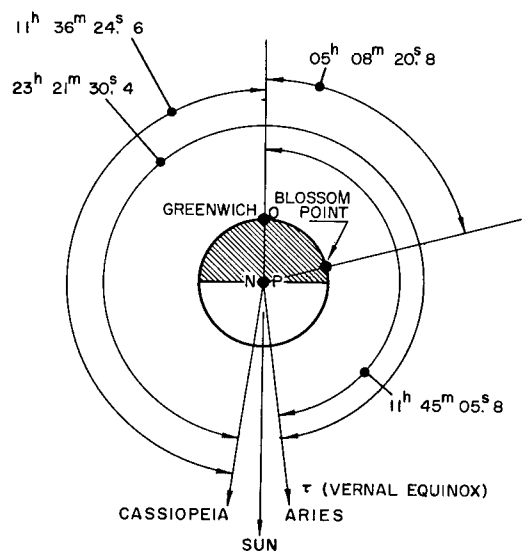

Figure 10 - Star-locating chart

of the American Ephemeris and Nautical Almanac, page 523. For $16^h\ 44^m\ 45^s.4$ the correction is $-02^m\ 44^s.6$. When this correction is taken into consideration the true mean solar time of transit of Cassiopeia over Blossom Point is $16^h\ 42^m\ 00^s.8$ U.T. To convert this time to local Eastern Standard Time it is necessary to subtract five hours since there are five time zones between Greenwich and Blossom Point. The local time of transit for Cassiopeia at Blossom Point on 19 March 1957 is therefore $11^h\ 42^m\ 00^s.8$ E.S.T.

System Measurement of Star Positions

With the Mark II Minitrack system a crossover occurs at every half-wavelength of phase difference. The times of crossovers other than the zero crossover can be computed for a star as follows:

$$\cos \alpha = \frac{S}{d} = \frac{n\lambda}{2d} = -\cos \delta \sin (\mathrm{LHA}),$$

where δ is the declination; $n = 0, \pm1, \pm2, \pm3, \pm4, \pm5$; and LHA is the "local hour angle" or angular distance from the local meridian of longitude to the star. Thus

$$\sin (\mathrm{LHA}) = \frac{-n\lambda}{2d \cos \delta}.$$

The 500-foot baseline used is 54.9020 wavelengths at 108 Mc. For Cassiopeia, the declination changes only negligibly from 1 January to 19 March, and the value at the former date, $58° 34'.4$, can be employed. Then

$$\sin \mathrm{LHA} = \frac{-n\lambda}{2(54.9020)(0.5214)}.$$

Thus the local hour angles may be computed for the five values of n, and the time value of each hour angle is the interval between the given crossover and the zero crossover:

$\frac{n\lambda}{2}$	sin(LHA)	LHA (arc)	LHA (sidereal time)	LHA (solar time)
±0.5	0.17466	1° 0' 3"	$4^m\ 0^s.2$	$3^m\ 59^s.5$
±1.0	0.034933	2° 0' 6"	8 0.4	7 59.1
±1.5	0.052399	3° 0' 13"	12 0.867	11 58.9
±2.0	0.069866	4° 0' 23"	16 1.533	15 58.9
±2.5	0.087332	5° 0' 37"	20 2.467	19 59.2

If the solar time intervals thus obtained are added algebraically to the zero crossover time, the results are the times for the preceding and succeeding crossovers. These calculated times may then be compared to the actual measured times, and the average difference will be the "tracking difference" for 19 March 1957:

UNCLASSIFIED

$\frac{n\lambda}{2}$	Measured Time	Calculated Time	Difference
-2	$11^h\ 25^m\ 47^s.2$	$11^h\ 26^m\ 01^s.9$	$-14^s.7$
-1.5	11 25 48.2	11 30 01.9	-13.7
-1	11 33 49.7	11 34 01.7	-12.0
-0.5	11 37 48.5	11 38 01.3	-12.8
0	11 41 43.7	11 42 00.8	-17.1
±0.5	11 45 41.1	11 46 00.3	-19.2
±1	11 49 55.7	11 49 59.9	-4.2
±1.5	11 53 26.3	11 53 59.7	-33.4
+2	11 58 10.6	11 57 59.7	+10.9
+2/5	12 01 30.0	12 02 00.0	-30.0
			$-146^s.2$
		Average:	$-\ 14^s.6$

The electrical integration delay referred to previously must be included in the analysis. The integrating circuit is a simple RC network, the phase delay of which is

$$\phi_d = -\arctan \frac{f}{f_c},$$

where f is the phase signal frequency and f_c is the filter cutoff frequency. The time delay due to this phase delay is

$$T_d = \frac{\phi_d}{360} \times \frac{1}{f}.$$

For small phase angles,

$$\phi_d = \frac{f}{f_c} \text{ radians.}$$

Then

$$T_d = \frac{f}{f_c \times 360} \times \frac{1}{f} \times 57.3 \text{ seconds}$$

$$= 5.3 \text{ seconds.}$$

It should be noted that the integration delay is independent of the phase signal frequency, hence of the angular rate and therefore of the declination of the source. This delay may be subtracted from the comparison figure directly; thus the average tracking difference for 19 March 1957 is -14.6 -5.3 = -19.9 seconds of time. To convert this time into arc it will suffice, because the interval is small, merely to use the expression for the diurnal motion of a star:

$$\omega = 15 \cos \delta \frac{\text{seconds of arc}}{\text{seconds of sidereal time}}.$$

The difference between sidereal and solar time can be ignored, again because of the small interval considered. Finally, since cos δ is practically unchanged by small changes in δ, the value δ_o can be used for δ. Thus for Cassiopeia

$$\omega = 15 \times 0.5214 = 7.82 \frac{\text{seconds of arc}}{\text{seconds of solar time}}$$

and the average tracking difference for 19 March 1957 is

$$-19.9 \times 7.82 = -155.6 \text{ seconds of arc.}$$

The daily tracking differences are plotted in Fig. 11 for three sources, Cassiopeia, Cygnus, and Taurus, during the period from 24 January to 10 April 1957; the tabulated data appear in Appendix A. The results show the average tracking difference for the three sources during this period to be: Cassiopeia, -114.6 seconds of arc; Cygnus, -80.0 seconds; and Taurus, -114.0 seconds. This tracking difference should not be considered an "error" in the ordinary sense; unequal line lengths or differences in antenna levels cause this difference, hence the necessity for external calibration. The average of the three tracking differences given above constitutes the calibration of the system.

To provide a check of the radio star calibration, the system was also calibrated by the technique used for the Prime Minitrack System, i.e., an aircraft-borne source with a flashing light photographed against a star background for precise location of the aircraft. This method is complicated but precise. The results for three angular positions of the aircraft, 20 degrees north, overhead, and 20 degrees south, which closely approximate the radio-star positions, compare in the following manner with the results of the radio-star calibration:

Aircraft Angular Position from Station	Aircraft Calibration	Radio Star Angular Position from Station	Radio Star Calibration	Calibration Difference
20° N	-101.4 sec of arc	Cass 20° 07' N	-114.6 sec of arc	-13.2 sec of arc
0°	-111.1 " " "	Cygn 2° 10' N	- 80.0 " " "	31.1 " " "
20° S	-152.7 " " "	Taur 16° 23' S	-114.0* " " "	38.7* " " "

The greatest excursion of the calibrating difference is slightly over 30 seconds of arc.* This is the anticipated accuracy of the system and indicates that the radio-star sources can successfully be used for station calibration.

RESULTS AND CONCLUSIONS

The zero reference line for the data shown in Fig. 11 is the average of the data taken over the period plotted. For Cassiopeia it is -114.6 seconds of arc, for Cygnus -80.0 seconds of arc, and for Taurus, -114.0 seconds of arc. Although the data fluctuate widely,

*It is believed that, during the first month of the observations, the signals from Taurus were refracted by an ionospheric "wedge effect." This effect can also be expected to displace the apparent position of a satellite from time to time during tracking operations, and constitutes one of the unavoidable difficulties of satellite radio tracking. If the observations believed to be so affected are discarded, the Taurus calibration becomes -130.9 seconds of arc, and the calibration difference 21.8 seconds of arc.

UNCLASSIFIED

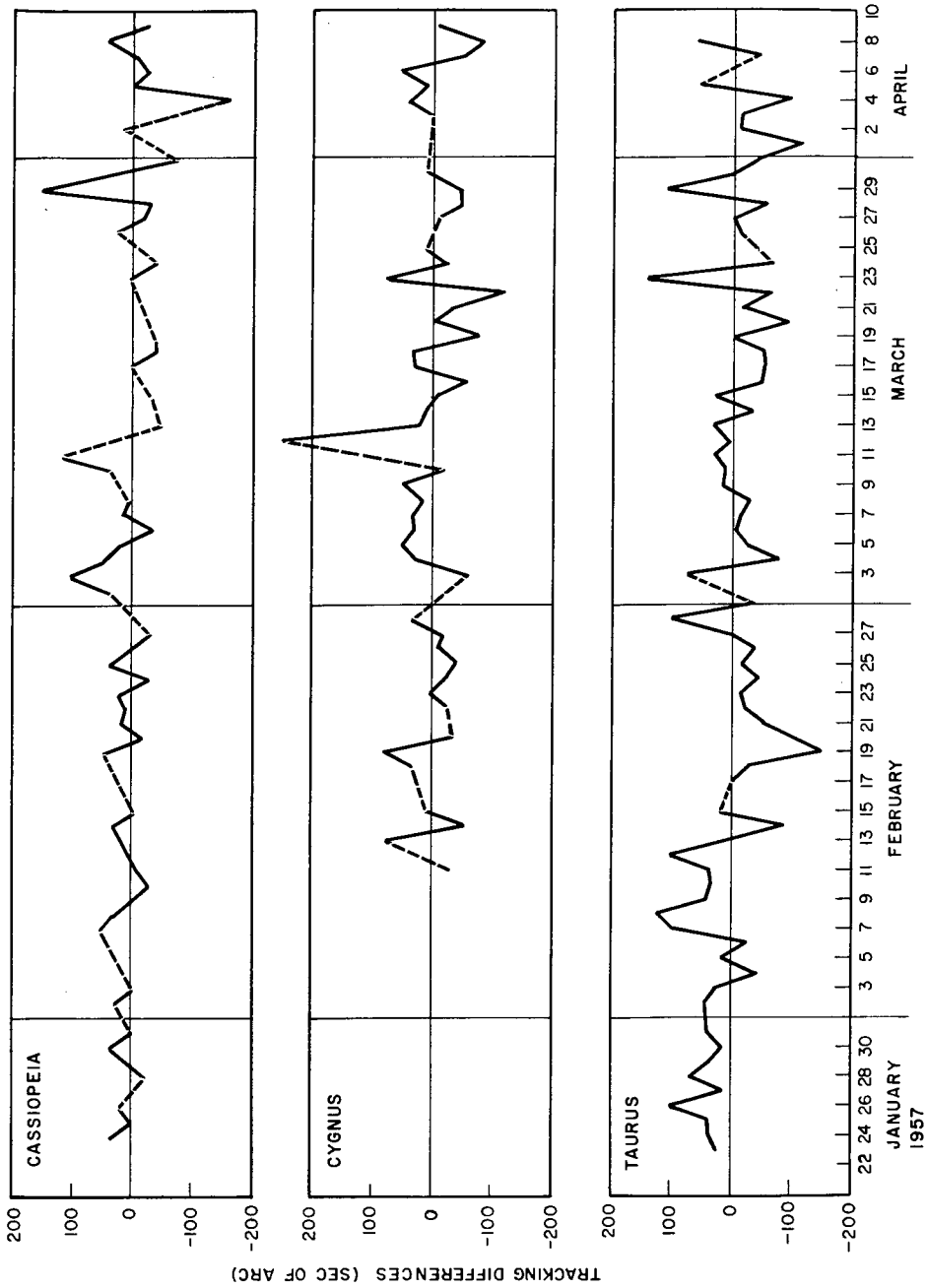

Figure 11 - Tracking differences for three sources from 24 January to 10 April 1957

the variations are apparently random so that a sufficiently long period of data should permit a calibration to an accuracy of better than 30 seconds of arc. An examination of the plots indicates that this calibrating period should be at least 20 days.

The daily tracking difference as used in the calibration procedure has been the average of the differences between the measured times of the ten crossovers and their respective computed times. Plots of these differences during daily star transits yield information concerning the rate and amplitude of the ionospheric fluctuations that occur in the hour or so during which the star is within the beam of the receiving antenna.

Figure 12 through 18 are typical plots of tracking differences versus crossover where the tracking difference is the difference between the computed and measured crossover times expressed in seconds of arc. The crossover designated zero is the one occurring nearest the computed time and the ones on either side are designated accordingly.

The solid curves are composed of straight lines connecting the data points (tracking differences) which occur at each crossover. The dashed lines are smoothed representations of the raw data. As was discussed previously, the crossovers are read with respect to a more or less arbitrarily chosen reference line close to the center of the recorded signals. However, it is difficult to find the exact center at times, and also this center sometimes changes with changes in the background radiation level. For this reason it was decided to maintain a particular reference line throughout the run. It might seem that the accuracy of the data analysis might suffer through this procedure, but very little actual deterioration is encountered. A reference line chosen too far to the left of the recorded track, for example, makes the crossover times occur too soon for traces moving from left to right, but an equal amount late in the opposite direction. Thus in the average the error virtually disappears. The dashed curve is the result of averaging each data point with its neighbor on each side; the end points, of course, are averaged with only one neighboring point. The dashed curve, therefore, has the reference line error removed and is thus a more realistic representation of the data.

As can be seen from the curves there is usually a great deal of fluctuation in the apparent position of the radio sources, even in time intervals of the order of a quarter-hour. It appears that at least a portion of the ionospheric layers are generally either in motion or changing in ion density. It is not inconceivable that the lower layers of the ionosphere might be affected by high-altitude winds, causing turbulence which could effectively create lenses that refract the signals passing through them.

In general the plotted data indicate that the variations are independent of the particular star or the time of day it transits, although the amount of data is not sufficient to justify too much credence in this. One notable exception occurred on 12 March, when a very strong sun spot caused intense geomagnetic activity. The fact that these shifts in apparent position seem to follow a more or less random distribution makes star calibrations appear even more attractive. Under these conditions it is only necessary to take a sufficient number of readings to permit the average system-derived positions to be close to the actual positions.

ACKNOWLEDGMENTS

This report could not have been written without the men who spent many hours in acquiring and analyzing the data. The efforts of the following men who performed these services are gratefully acknowledged:

Thomas M. Roth Jr. . . . . Army Map Service
Norman J. Cizek . . . . . Army Map Service
Edmond J. Habib . . . . . Naval Research Laboratory
William B. Moriarty . . . . . Naval Research Laboratory
John B. Martin . . . . . Naval Research Laboratory

UNCLASSIFIED

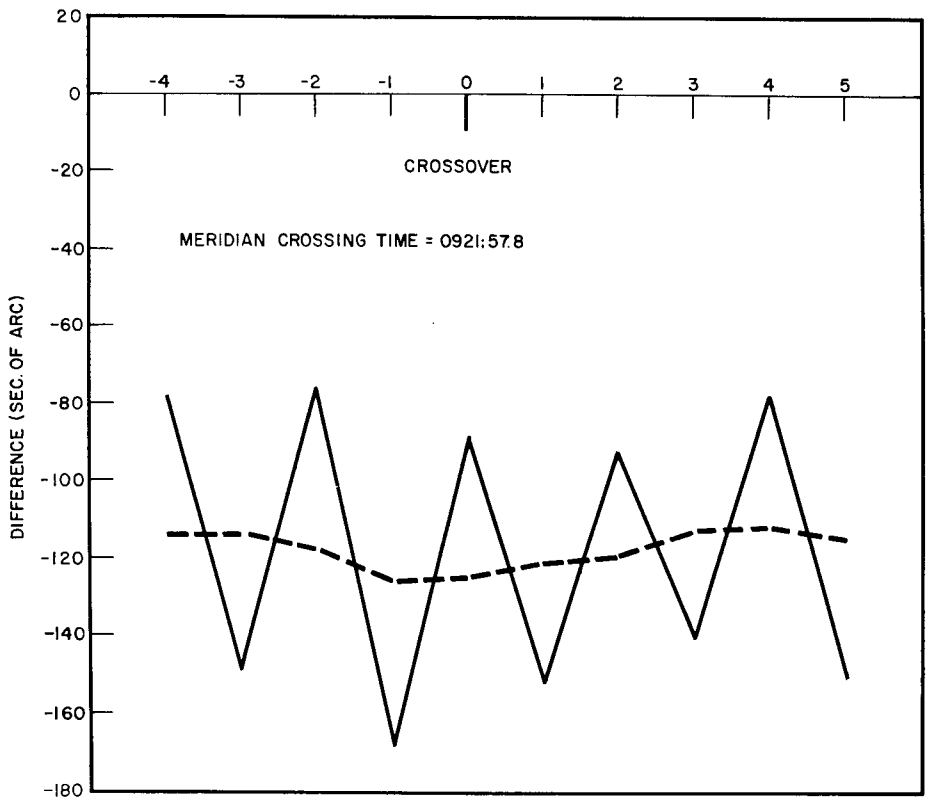

Figure 12 - Tracking differences for Cygnus, 3 March 1957

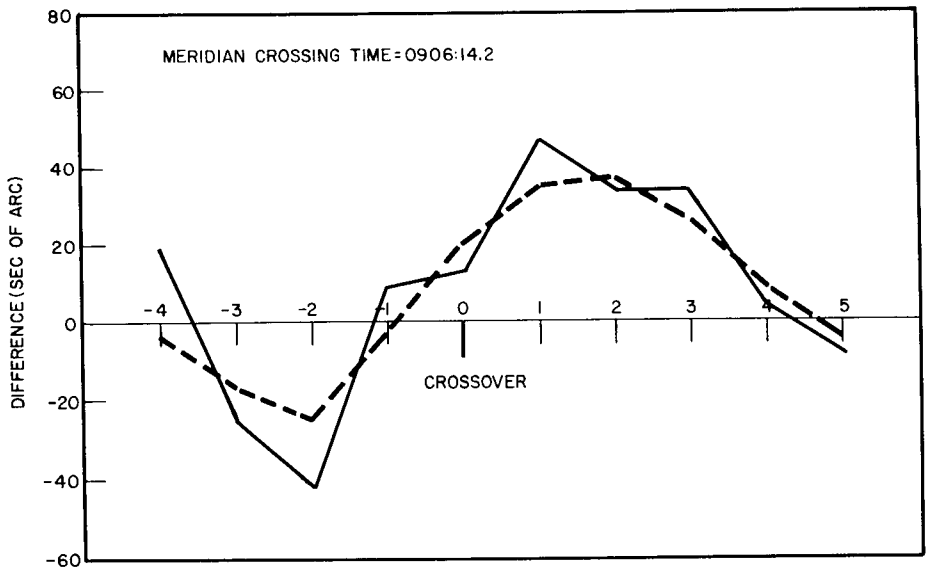

Figure 13 - Tracking differences for Cygnus, 7 March 1957

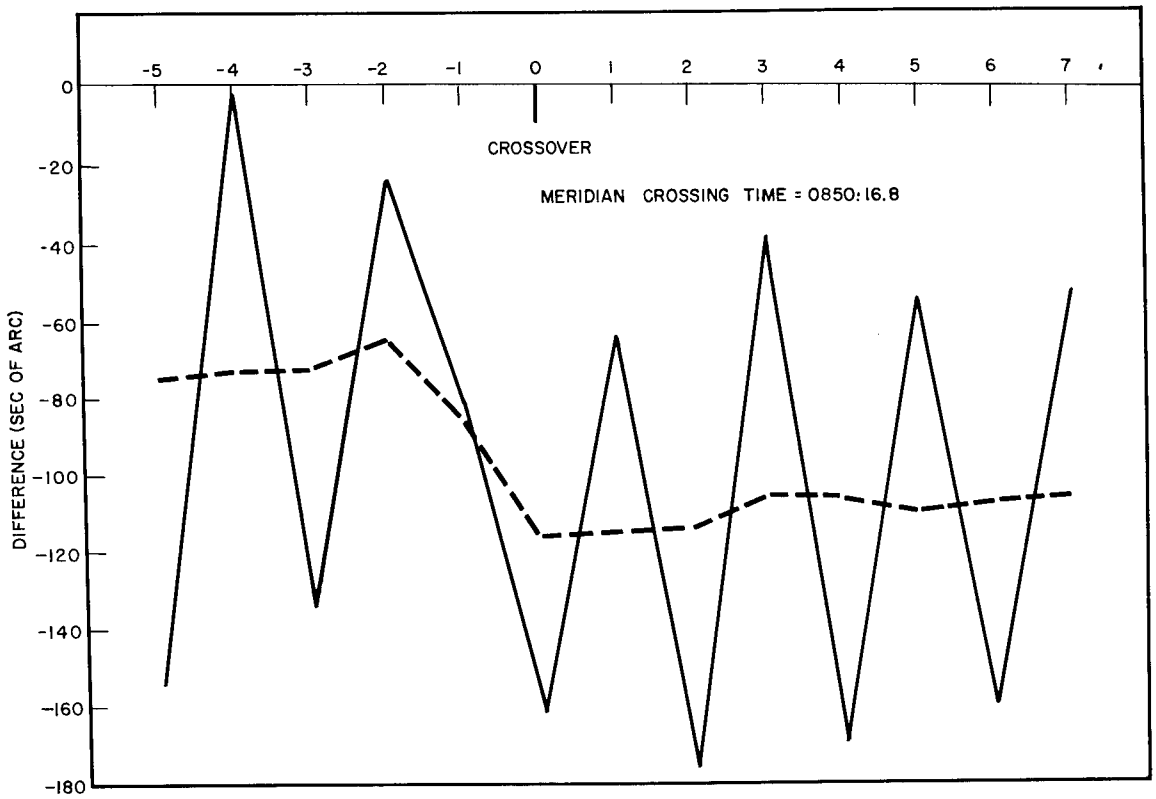

Figure 14 - Tracking differences for Cygnus, 11 March 1957

UNCLASSIFIED

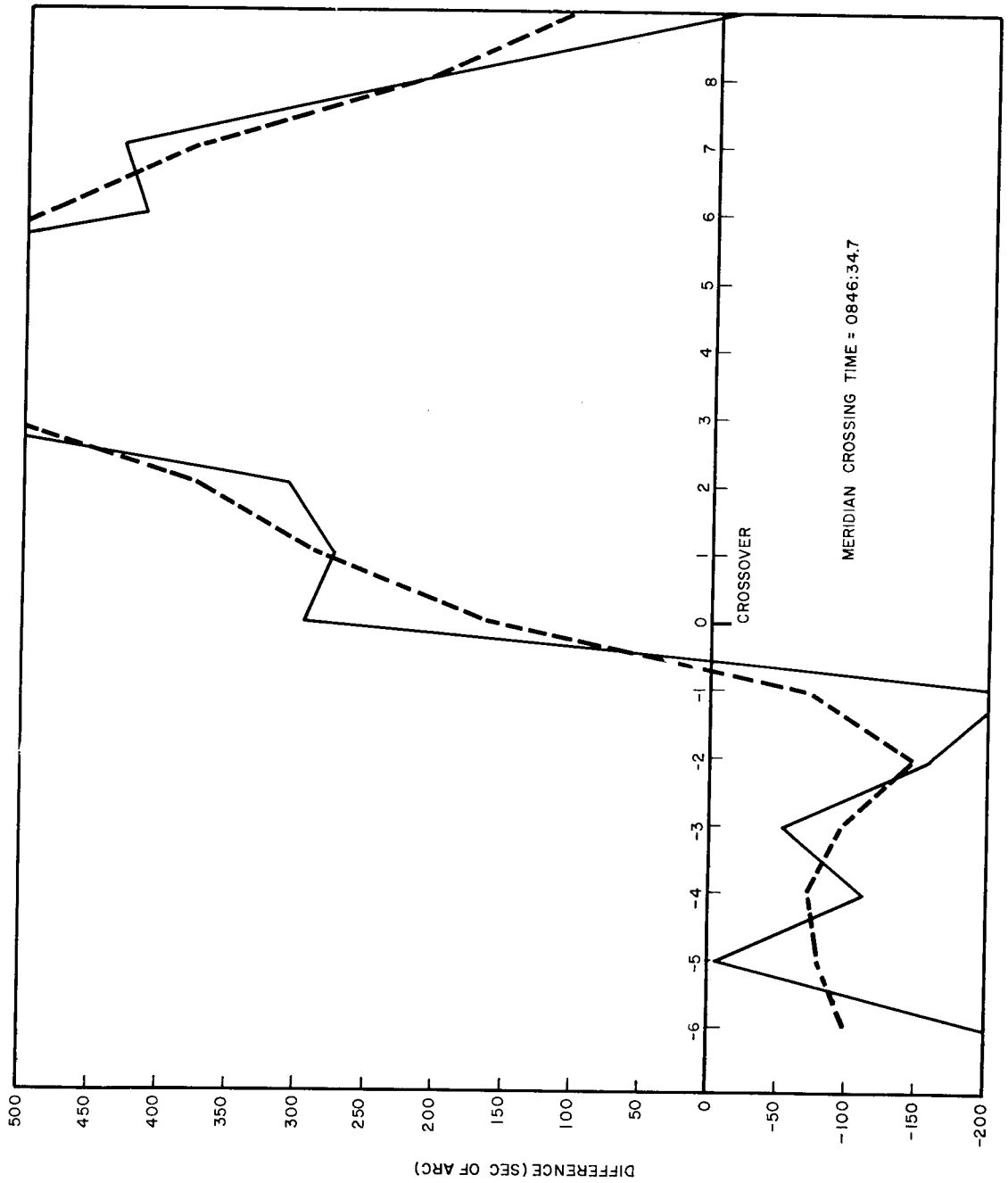

Figure 15 - Tracking differences for Cygnus, 12 March 1957

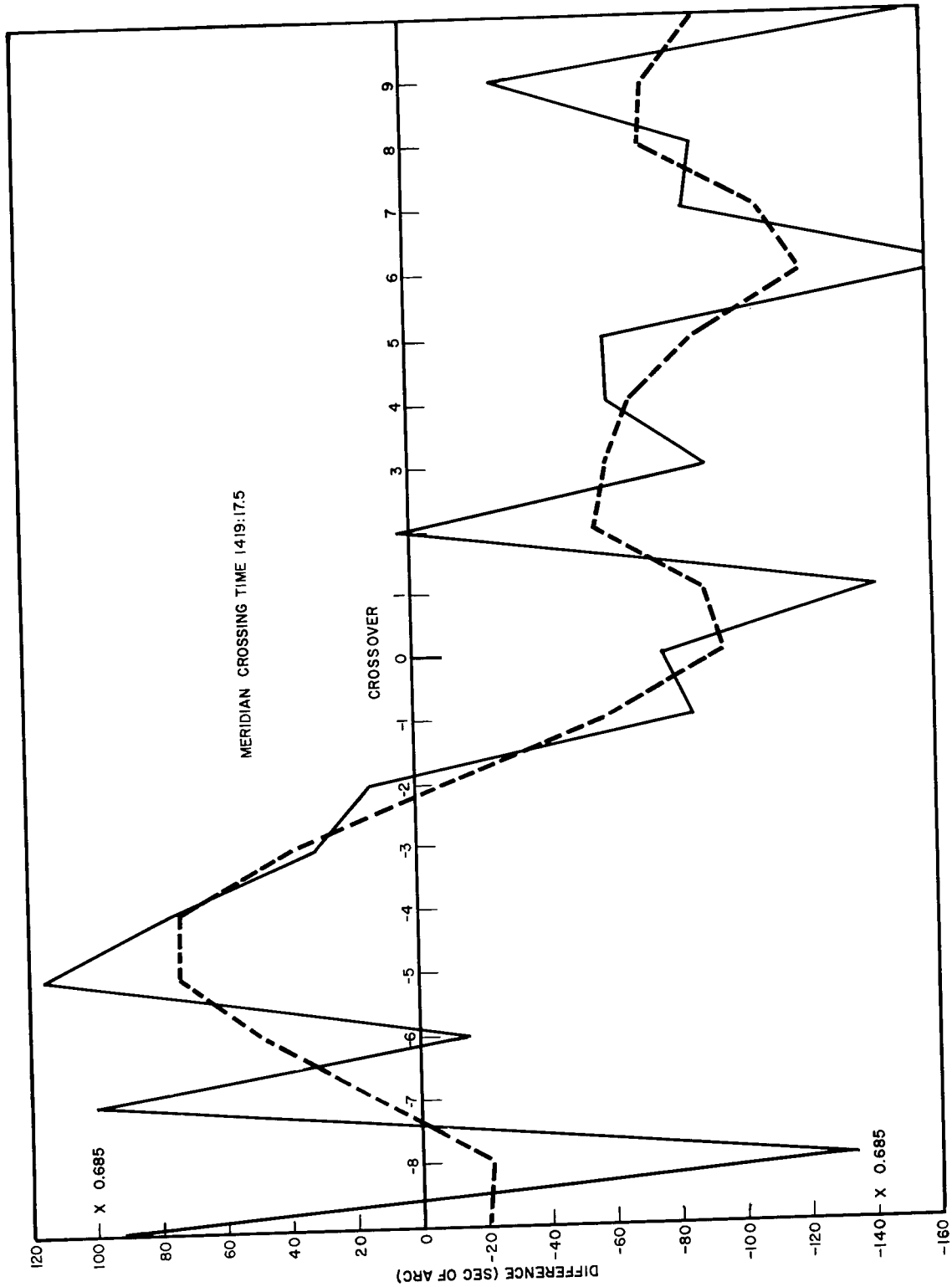

Figure 16 - Tracking differences for Cassiopeia, 7 February 1957

UNCLASSIFIED

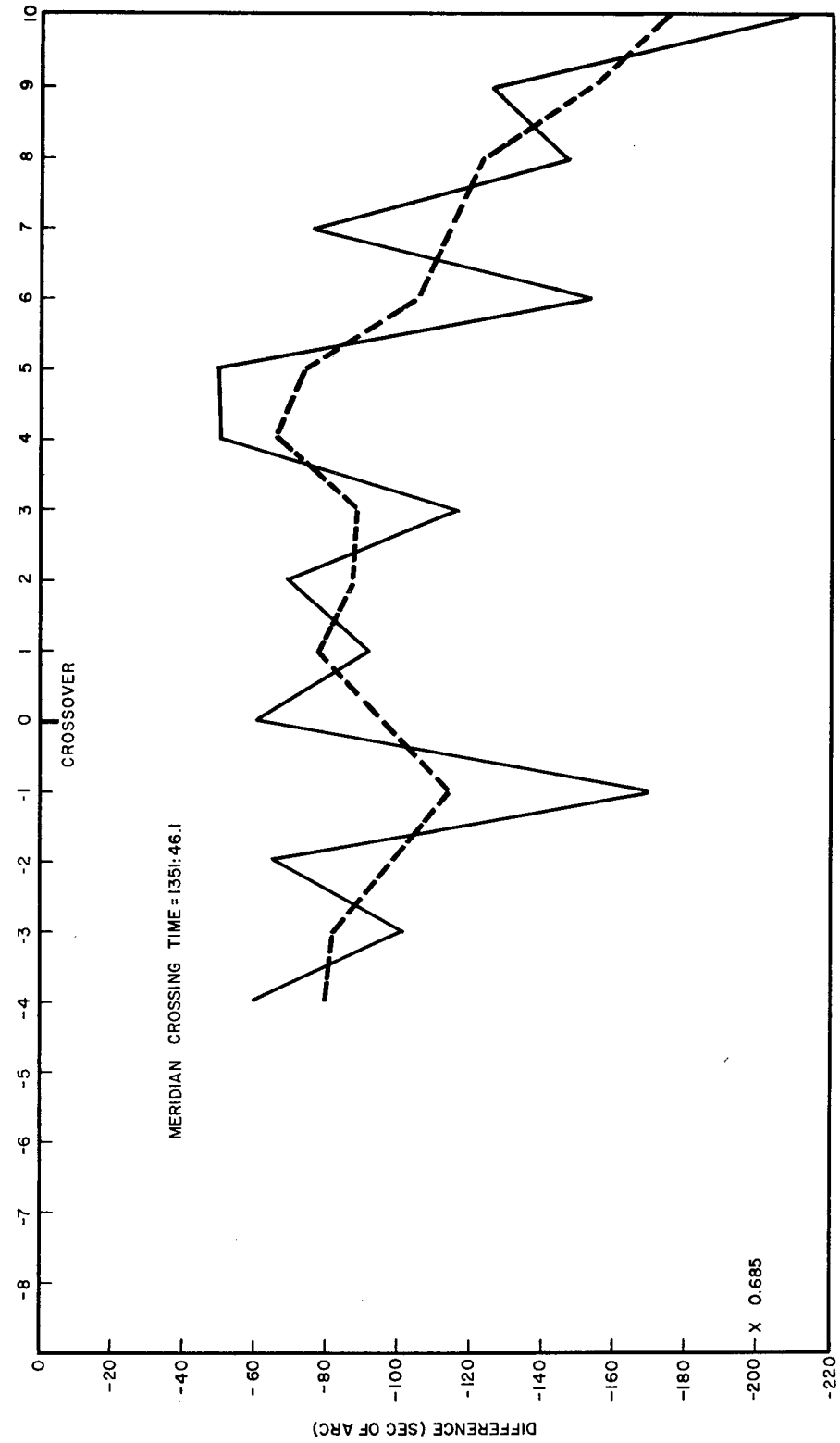

Figure 17 - Tracking differences for Cassiopeia, 14 February 1957

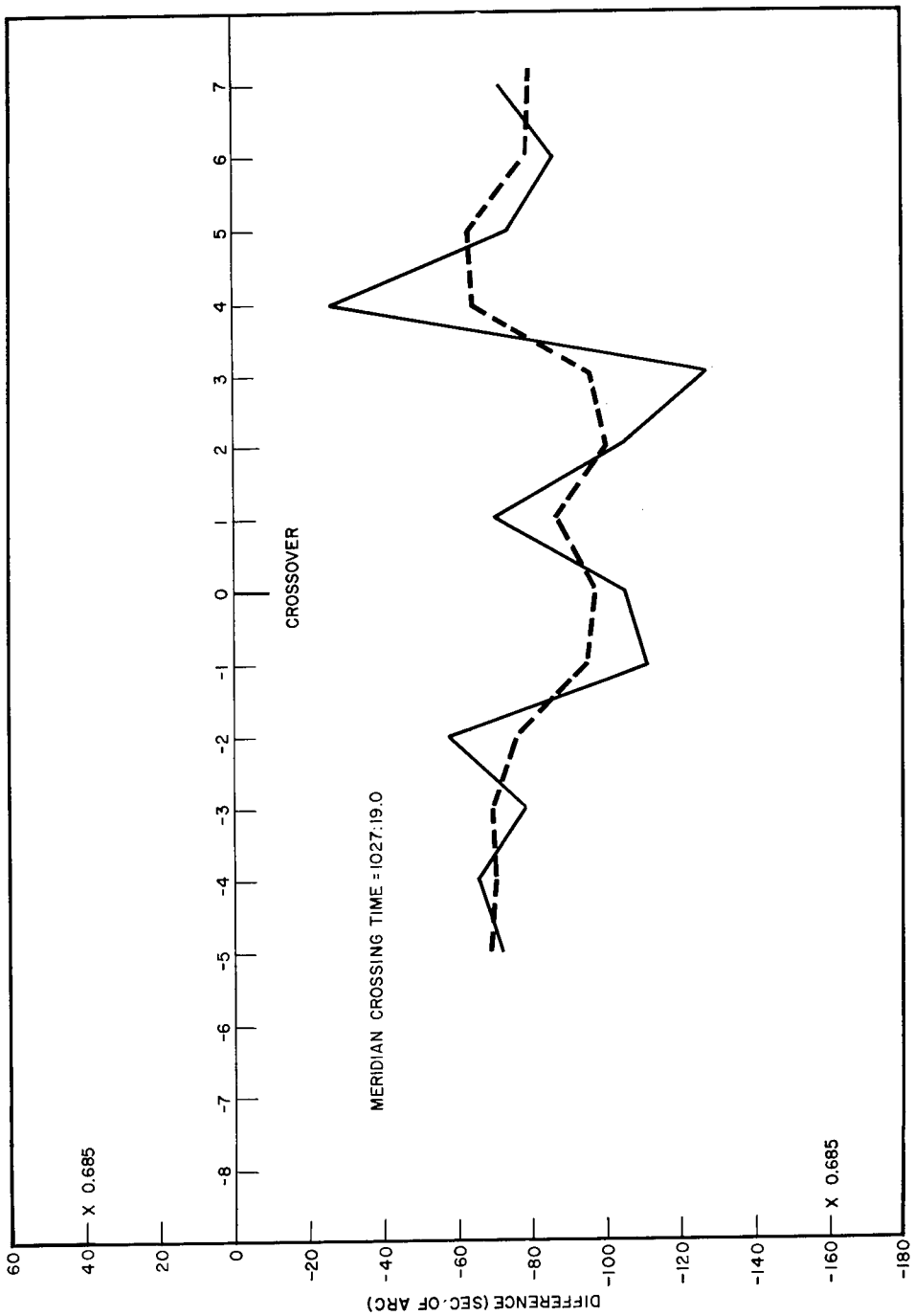

Figure 18 - Tracking differences for Cassiopeia, 7 April 1957

UNCLASSIFIED

Appendix A

DAILY TRACKING DATA FOR CASSIOPEIA, CYGNUS, AND TAURUS, 24 JANUARY - 10 APRIL 1957

MARK II CASSIOPEIA DATA - BLOSSOM POINT

(1 sec of time = 7.82 Sec of Arc)

Date (1957)	Corrected* Tracking Difference (Sec of Time)	Corrected* Tracking Difference (Sec of Arc)	Deviation from Mean (Sec of Arc)
24 Jan.	-10.66	- 83.36	+ 31.23
25 "	-14.70	-114.95	- .36
26 "	-12.20	- 95.40	+ 19.19
27 "	--	--	--
28 "	-17.59	-137.55	- 22.96
29 "	-13.81	-107.99	+ 6.60
30 "	-10.10	- 78.98	+ 35.61
31 "	-14.90	-116.51	- 1.92
1 Feb.	--	--	--
2 "	-11.20	- 87.58	+ 27.01
3 "	-14.70	-114.95	- 0.36
4 "	--	--	--
5 "	--	--	--
6 "	--	--	--
7 "	8.30	- 64.91	+ 49.68
8 "	-10.78	- 84.30	+ 30.29
9 "	-14.90	-116.52	- 1.93
10 "	-18.50	-144.67	- 30.08
11 "	-16.30	-127.47	- 12.88
12 "	-14.90	-116.52	- 1.93
13 "	-12.60	- 98.54	+ 16.05
14 "	-10.90	- 85.24	+ 29.35
15 "	-15.50	-121.21	- 6.62
16 "	--	--	--
17 "	--	--	--
18 "	--	--	--
19 "	- 8.81	- 68.89	+ 45.70
20 "	-17.21	-134.58	- 19.99
21 "	-12.40	- 96.97	+ 17.62
22 "	-12.53	- 97.98	+ 16.61
23 "	--	--	--
24 "	-12.01	- 93.92	+ 20.67
25 "	-18.53	-144.90	- 30.31
26 "	-10.05	- 78.59	+ 36.00
27 "	-14.85	-116.13	- 1.54
28 "	-17.59	-137.55	- 22.96
1 March	--	--	--
2 "	- 9.94	- 77.73	+ 36.86
3 "	-16.00	- 12.51	+102.08
4 "	- 8.87	- 69.36	+ 45.23
5 "	-11.98	- 93.68	+ 20.91
6 "	-19.00	-148.58	- 33.99
7 "	-12.74	- 99.63	+ 14.96
8 "	-13.97	-109.24	+ 5.35
9 "	--	--	--
10 "	-10.26	- 80.23	+ 34.36
11 "	+ .29	+ 2.26	+116.85
12 "	--	--	--
13 "	-20.57	160.86	- 46.27
14 "	--	--	--
15 "	-18.82	147.17	- 32.58
16 "	--	--	--
17 "	-14.51	113.47	+ 1.12
18 "	-19.76	154.52	- 39.93
19 "	-19.9	155.6	- 41.01
20 "	--	--	--
21 "	--	--	--
22 "	--	--	--
23 "	-13.95	109.09	+ 5.50
24 "	-19.98	156.24	- 41.65
25 "	--	--	--
26 "	-11.09	86.72	+ 27.87
27 "	-17.02	133.10	- 18.51
28 "	-18.21	142.40	- 27.81
29 "	+ 4.74	+ 37.07	+151.66
30 "	- 8.16	63.81	+ 50.78
31 "	-23.10	180.64	- 66.05
1 April	--	--	--
2 "	-12.00	93.84	+ 20.75
3 "	--	--	--
4 "	-35.40	276.83	-162.24
5 "	-14.38	112.45	+ 2.14
6 "	-17.86	139.67	- 25.08
7 "	-15.33	119.88	- 5.29
8 "	- 9.34	73.04	+ 41.55
9 "	-17.77	138.96	- 24.37
		Mean Value = -114.54	RMS Value = ±46.36

*Corrected for electrical integration delay of 5.3 sec of time.

UNCLASSIFIED

MARK II CYGNUS DATA - BLOSSOM POINT

(1 sec of time = 11.39 Sec of Arc)

Date (1957)	Corrected* Tracking Difference		Deviation from Mean
	(Sec of Time)	(Sec of Arc)	(Sec of Arc)
9 Feb.	--	--	--
10 "	--	--	--
11 "	- 9.40	-107.07	- 27.06
12 "	--	--	--
13 "	- 5.74	- 65.38	+ 74.27
14 "	-12.14	-138.27	- 58.26
15 "	- 6.11	- 69.59	+ 10.42
16 "	--	--	--
17 "	--	--	--
18 "	- 3.98	- 45.33	- 34.68
19 "	- .53	- 6.05	+ 73.98
20 "	-10.23	-116.52	- 36.51
21 "	--	--	--
22 "	- 9.04	-102.97	- 22.96
23 "	- 7.37	- 83.94	- 3.93
24 "	- 8.99	-102.40	- 22.39
25 "	-10.50	-119.60	- 39.59
26 "	- 7.93	- 90.32	- 10.31
27 "	- 8.68	- 98.87	- 18.86
28 "	- 4.63	- 52.73	+ 27.28
1 March	--	--	--
2	--	--	--
3 "	-15.29	-143.40	- 63.39
4 "	- 4.77	- 54.33	+ 25.68
5 "	- 2.78	- 31.66	+ 48.35
6 "	- 4.50	- 51.26	+ 28.75
7 "	- 4.33	- 49.32	+ 30.69
8 "	- 5.77	- 65.72	+ 14.29
9 "	- 2.86	- 32.58	+ 47.43
10 "	- 8.68	- 98.87	- 18.86
11 "	--	--	--
12 "	+14.28	+162.65	+242.66
13 "	- 5.30	- 60.38	+ 19.63
14 "	- 6.41	- 73.01	+ 7.00
15 "	- 8.05	- 91.69	- 11.68
16 "	-12.42	-141.46	- 61.45
17 "	- 4.36	- 49.66	+ 30.35
18 "	- 4.18	- 47.61	+ 32.40
19 "	-13.95	-158.89	- 78.88
20 "	- 7.27	- 82.81	- 2.80
21 "	- 9.72	-110.71	- 30.70
22 "	-17.84	-203.20	-123.19
23 "	- .49	- 5.58	+ 74.43
24 "	- 9.20	-104.79	- 24.78
25 "	- 5.95	- 67.77	+ 12.24
26 "	--	--	--
27 "	- 7.94	- 90.44	- 10.43
28 "	-11.34	-129.16	- 49.15
29 "	-10.64	-121.19	- 41.18
30 "	- 6.14	- 69.93	10.08
31 "	--	--	--
1 April	--	--	--
2 "	--	--	--
3 "	- 7.00	- 79.73	+ 0.28
4 "	- 3.28	- 37.36	+ 42.65
5 "	- 5.96	- 67.88	- 12.13
6 "	- 2.30	- 26.20	- 53.81
7 "	-11.26	-128.25	- 48.24
8 "	-14.15	-161.17	- 81.16
9 "	- 7.73	- 88.04	- 8.03
		Mean Value = - 80.01	RMS Value = ± 55.6

*Corrected for electrical integration delay of 5.2 sec of time.

MARK II TAURUS DATA - BLOSSOM POINT

(1 sec of time = 13.91 Sec of Arc)

Date (1957)	Corrected* Tracking Difference (Sec of Time)	Corrected* Tracking Difference (Sec of Arc)	Deviation from Mean (Sec of Arc)
23 Jan.	- 6.32	- 87.9	+ 26.1
24 "	- 5.75	- 80.0	+ 34.0
25 "	- 5.31	- 73.9	+ 40.1
26 "	- 1.37	- 19.1	+ 94.9
27 "	- 7.13	- 99.2	+ 14.8
28 "	- 3.54	- 49.2	+ 64.8
29 "	- 5.77	- 80.3	+ 33.7
30 "	- 7.05	- 98.1	+ 15.9
31 "	- 5.54	- 77.1	+ 36.9
1 Feb.	- 5.33	- 74.1	+ 39.9
2 "	- 5.21	- 72.5	+ 41.5
3 "	- 6.55	- 91.1	+ 22.9
4 "	-11.43	-159.0	- 45.0
5 "	- 7.15	- 99.5	+ 14.5
6 "	-10.15	-141.2	- 27.2
7 "	- 1.23	- 17.1	+ 96.9
8 "	+ 0.63	+ 8.8	+122.8
9 "	- 5.52	- 76.8	+ 37.2
10 "	- 5.70	- 79.3	+ 34.7
11 "	- 5.43	- 75.5	+ 38.5
12 "	- 0.81	- 11.3	+102.7
13 "	- 7.15	- 99.5	+ 14.5
14 "	-14.36	-199.7	- 85.7
15 "	- 6.78	- 94.3	+ 19.7
16 "	--	--	--
17 "	- 8.43	-117.3	- 3.3
18 "	-10.29	-143.1	- 29.1
19 "	-19.03	-264.7	-150.7
20 "	--	--	--
21 "	-12.15	-169.0	- 55.0
22 "	-10.06	-139.9	- 25.9
23 "	- 9.52	-132.4	- 18.4
24 "	-11.66	-162.2	- 48.2
25 "	- 9.64	-134.1	- 20.1
26 "	-11.14	-155.0	- 41.0
27 "	- 8.29	-115.3	- 1.3
28 "	- 1.12	- 15.6	+ 98.4
1 March	-10.85	-150.9	- 36.9
2 "	--	--	--
3 "	- 3.20	- 44.5	+ 69.5
4 "	-13.95	-194.0	- 80.0
5 "	-10.15	-141.2	- 27.2
6 "	- 8.86	-123.2	- 9.2
7 "	- 9.35	-130.1	- 16.1
8 "	-10.49	-145.9	- 31.9
9 "	- 6.98	- 97.1	+ 16.9
10 "	- 7.40	-102.9	+ 11.1
11 "	- 6.13	- 85.3	+ 28.7
12 "	- 8.03	-111.7	+ 2.3
13 "	- 6.20	- 86.2	+ 27.8
14 "	-11.01	-153.1	- 39.1
15 "	- 6.27	- 87.2	+ 26.8
16 "	-11.84	-164.7	- 50.7
17 "	-12.16	-169.1	- 55.1
18 "	-11.94	-166.1	- 52.1
19 "	- 8.52	-118.5	- 4.5
20 "	-14.88	-207.0	- 93.0
21 "	-10.08	-140.2	- 26.2
22 "	-12.72	-176.9	- 62.9
23 "	+ 1.76	+ 24.5	+138.5
24 "	-12.79	-177.9	- 63.9
25 "	--	--	--
26 "	- 9.17	-127.6	- 13.6
27 "	- 8.31	-115.6	- 1.6
28 "	-12.49	-173.7	- 59.7
29 "	- 0.57	- 7.9	+106.1
30 "	- 8.47	-117.8	- 3.8
31 "	-11.25	-156.5	- 42.5
1 April	-16.32	-227.0	-113.0
2 "	- 9.12	-126.9	- 12.9
3 "	- 9.22	-128.3	- 14.3
4 "	-14.73	-204.9	- 90.9
5 "	- 4.17	- 58.0	+ 56.0
6 "	--	--	--
7 "	-11.18	-155.5	- 41.5
8 "	- 4.01	- 55.8	+ 58.2
		Mean Value = -114.0	RMS Value = ± 44.43

*Corrected for electrical integration delay of 5.2 sec of time.